Enhanced nonreciprocal effects in magnetoplasmonic systems supporting simultaneously localized and propagating plasmons

R. Kekesi,[1*] D. Martín-Becerra,[1] D. Meneses-Rodríguez,[1,2] F. García-Pérez,[1] A. Cebollada[1] and G. Armelles[1,3]

[1] *Instituto de Microelectrónica de Madrid (CNM-CSIC), Isaac Newton 8, PTM, E-28760 Tres Cantos, Madrid, Spain*
[2] *Department of Applied Physics, CINVESTAV-IPN, Antigua Carretera a Progreso, Km 6, Mérida, Yuc. 97310, Mexico*
[3]*gaspar@imm.cnm.csic.es*
renata.kekesi@outlook.com

Abstract: Perforated magnetoplasmonic Au/Co/Au multilayers support both localized and propagating surface plasmon resonances. The presence of holes produces an enhancement of the magnetic field modulation of the propagating surface plasmon wavevector with respect to the isostructural continuous film in the spectral region corresponding to the hole associated localized plasmon resonance. This is due to the increased electromagnetic field in the surrounding area of the resonant hole, and the subsequent additional contribution to the magnetic modulation of the continuous film. This novel concept that gives rise to enhanced magnetic field induced nonreciprocal effects can be of interest in the development of innovative platforms for sensing applications, optical isolators and modulators.

OCIS codes: (210.3820) Magneto-optical materials; (230.3810) Magneto-optic systems; (240.6680) Surface plasmons; (250.5403) Plasmonics; (260.3910) Metal optics.

References and links

1. R. J. Potton, "Reciprocity in optics," Rep. Prog. Phys. **67**(5), 717–754 (2004).
2. H. Shimizu, "Semiconductor optical isolators for integrated optics," Proc. SPIE **8813**, 88132C (2013).
3. V. Zayets, H. Saito, K. Ando, and S. Yuasa, "Optical isolator utilizing surface plasmons," Materials **5**(12), 857–871 (2012).
4. X. Zang and C. Jiang, "Edge mode in nonreciprocal photonic crystal waveguide: manipulating the unidirectional electromagnetic pulse dynamically," J. Opt. Soc. Am. B **28**(3), 554–557 (2011).
5. J. B. González-Díaz, A. Garcia-Martin, G. Armelles, J. M. Garcia-Martin, C. Clavero, A. Cebollada, R. A. Lukasew, J. R. Skuza, D. P. Kumah, and R. Clarke, "Surface-magnetoplasmon nonreciprocity effects in noble-metal/ferromagnetic heterostructures," Phys. Rev. B **76**(15), 153402 (2007).
6. D. Nikolova and A. J. Fisher, "Switching and propagation of magnetoplasmon polaritons in magnetic slot waveguides and cavities," Phys. Rev. B **88**(12), 125136 (2013).
7. J. Y. Chin, T. Steinle, T. Wehlus, D. Dregely, T. Weiss, V. I. Belotelov, B. Stritzker, and H. Giessen, "Nonreciprocal plasmonics enables giant enhancement of thin-film Faraday rotation," Nat Commun **4**, 1599 (2013).
8. Y. M. Strelniker and D. J. Bergman, "Strong angular magneto-induced anisotropy of Voigt effect in metal-dielectric metamaterials with periodic nanostructures," Phys. Rev. B **89**(12), 125312 (2014).
9. G. Mathew, C. Bhagyaraj, A. Babu, and V. Mathew, "Effect of gyrotropic substrates on the surface plasmon polaritons guided by metal films of finite width," J. Lightwave Technol. **30**(2), 273–278 (2012).
10. M. Khatir and N. Granpayeh, "An ultra compact and high speed magneto-optic surface plasmon switch," J. Lightwave Technol. **31**(7), 1045–1054 (2013).
11. A. N. Kalish, D. O. Ignatyeva, V. I. Belotelov, L. E. Kreilkamp, A. Akimov, A. V. Gopal, M. Bayer, and A. P. Sukhorukov, "Transformation of mode polarization in gyrotropic plasmonic waveguides," Laser Phys. **24**(9), 094006 (2014).
12. H. H. Wu and Y. C. Lan, "Magnetic lenses of surface magnetoplasmons in semiconductor–glass waveguide arrays," Appl. Phys. Express **7**(3), 032203 (2014).
13. G. Mathew and V. Mathew, "Tunable surface plasmon polaritons in metal-strip waveguides with magnetized semiconductor substrates in Voigt configuration," Semicond. Sci. Technol. **27**(5), 055010 (2012).

14. B. Sepúlveda, A. Calle, L. M. Lechuga, and G. Armelles, "Highly sensitive detection of biomolecules with the magneto-optic surface-plasmon-resonance sensor," Opt. Lett. **31**(8), 1085–1087 (2006).
15. M. G. Manera, G. Montagna, E. Ferreiro-Vila, L. González-García, J. R. Sánchez-Valencia, A. R. González-Elipe, A. Cebollada, J. M. Garcia-Martin, A. Garcia-Martin, G. Armelles, and R. Rella, "Enhanced gas sensing performance of TiO2 functionalized magneto-optical SPR sensors," J. Mater. Chem. **21**(40), 16049 (2011).
16. K. H. Chou, E. P. Lin, T. C. Chen, C. H. Lai, L. W. Wang, K. W. Chang, G. B. Lee, and M. C. M. Lee, "Application of strong transverse magneto-optical Kerr effect on high sensitive surface plasmon grating sensors," Opt. Express **22**(16), 19794–19802 (2014).
17. S. David, C. Polonschii, C. Luculescu, M. Gheorghiu, S. Gáspár, and E. Gheorghiu, "Magneto-plasmonic biosensor with enhanced analytical response and stability," Biosens. Bioelectron. **63**(15), 525–532 (2015).
18. K. Kämpf, S. Kübler, F. W. Herberg, and A. Ehresmann, "Magneto-optic surface plasmon resonance optimum layers: simulations for biological relevant refractive index changes," J. Appl. Phys. **112**(3), 034505 (2012).
19. D. Regatos, D. Fariña, A. Calle, A. Cebollada, B. Sepulveda, G. Armelles, and L. M. Lechuga, "Au/Fe/Au multilayer transducers for magneto-optic surface plasmon resonance sensing," J. Appl. Phys. **108**(5), 054502 (2010).
20. G. Armelles, A. Cebollada, A. García-Martín, and M. U. González, "Magnetoplasmonics: combining magnetic and plasmonic functionalities," Adv. Opt. Mater. **1**(1), 10–35 (2013).
21. V. Bonanni, S. Bonetti, T. Pakizeh, Z. Pirzadeh, J. Chen, J. Nogués, P. Vavassori, R. Hillenbrand, J. Åkerman, and A. Dmitriev, "Designer magnetoplasmonics with nickel nanoferromagnets," Nano Lett. **11**(12), 5333–5338 (2011).
22. J. F. Torrado, J. B. Gonzalez-Diaz, A. García-Martín, and G. Armelles, "Unraveling the relationship between electromagnetic field intensity and the magnetic modulation of the wave vector of coupled surface plasmon polaritons," New J. Phys. **15**(7), 075025 (2013).
23. D. Martín-Becerra, J. B. González-Díaz, V. V. Temnov, A. Cebollada, G. Armelles, T. Thomay, A. Leitenstorfer, R. Bratschitsch, A. García-Martín, and M. U. González, "Enhancement of the magnetic modulation of surface plasmon polaritons in Au/Co/Au films," Appl. Phys. Lett. **97**(18), 183114 (2010).
24. C. Clavero, K. Yang, J. R. Skuza, and R. A. Lukaszew, "Magnetic field modulation of intense surface plasmon polaritons," Opt. Express **18**(8), 7743–7752 (2010).
25. H. T. Huang, T. R. Ger, Y. R. Xu, C. Y. Huang, K. T. Liao, J. Y. Lai, J. Y. Chen, C. H. Chen, and Z. H. Wei, "Surface plasmon induced enhancement with magneto-optical layer," J. Appl. Phys. **115**(17), 17E313 (2014).
26. J. F. Torrado, J. B. González-Díaz, M. U. González, A. García-Martín, and G. Armelles, "Magneto-optical effects in interacting localized and propagating surface plasmon modes," Opt. Express **18**(15), 15635–15642 (2010).
27. J. Prikulis, P. Hanarp, L. Olofsson, D. Sutherland, and M. Käll, "Optical spectroscopy of nanometric holes in thin gold films," Nano Lett. **4**(6), 1003–1007 (2004).
28. T. Rindzevicius, Y. Alaverdyan, B. Sepulveda, T. Pakizeh, M. Käll, R. Hillenbrand, J. Aizpurua, and F. J. García de Abajo, "Nanohole Plasmons in Optically Thin Gold Films," J. Phys. Chem. C **111**(3), 1207–1212 (2007).
29. R. Kekesi, D. Meneses-Rodríguez, F. Garcia-Pérez, M. U. Gonzalez, A. Garcia-Martín, A. Cebollada, and G. Armelles, "The effect of holes in the dispersion relation of propagative surface plasmon modes of nanoperforated semitransparent metallic films," J. Appl. Phys. **116**(13), 134306 (2014).</jrn>
30. H. Fredriksson, Y. Alaverdyan, A. Dmitriev, C. Langhammer, D. Sutherland, M. Zäch, and B. Kasemo, "Hole–mask colloidal lithography," Adv. Mater. **19**(23), 4297–4302 (2007).
31. F. J. García de Abajo, J. J. Sáenz, I. Campillo, and J. S. Dolado, "Site and lattice resonances in metallic hole arrays," Opt. Express **14**(1), 7–18 (2006).

1. Introduction

A system whose optical response is different for counter-propagating light–beams is called nonreciprocal [1]. Nonreciprocity plays a very important role in the development of a large variety of unidirectional devices, like for example optical isolators, as well as in sensing applications [2–4]. A standard method to induce nonreciprocity is to apply an external magnetic field, for example, in a magneto-optical (MO) active medium, where the wavevector of circularly polarized light propagating along the direction of the applied magnetic field depends on the direction of propagation. On the other hand, a magnetic field applied in the sample plane and perpendicular to the Surface Plasmon (SP) propagation direction modifies the wavevector of the SP in such a way that, for the same frequency, SP's propagating in opposite directions have different wavevectors [5–8]. This magnetic field induced modification of the SP wavevector, has found applications in the development of different SP devices such as isolators [9–13] or sensors [14–19].

A way to reduce the magnetic field needed to change the SP wavevector inducing nonreciprocal effects is to incorporate ferromagnetic materials into the plasmonic structure [20,21]. In these magnetoplasmonic systems, nonreciprocal effects are proportional to the electromagnetic field distribution in the MO active component [22], and different strategies

have been followed to enhance these effects by electromagnetic field distribution engineering [23–25].

A way to provide with a further control on nonreciprocal properties is to design structures where, in addition to propagating plasmons, localized plasmon modes are also incorporated. This has been done for example by combining Au/Co/Au continuous films with Au nanodisks which, to preserve the localized nature of their resonances, were separated from the continuous films with a dielectric spacer [26]. It was found that the interaction between localized and propagating plasmon modes gave rise to a reduction of the SP magnetic modulation. In this case, two aspects contributed in a negative way to the plasmon modulation: the elements that are responsible for the generation of the localized and propagating modes were spatially separated and one of them (the Au disks) was not MO active.

To circumvent these two drawbacks, in the present work we propose the use of a nanoperforated Au/Co/Au continuous film (from now on, membrane). In this system the inter-hole continuous part of the membrane supports propagating plasmons and the holes are responsible for the localized resonances [27,28]. Moreover, since the hole-associated localized modes are due to the currents generated in the metallic region around them, the subsequent resonance enhanced EM (electromagnetic) field occurs in a MO active region (the metal). As a consequence, we will show how indeed, in the spectral region where the hole associated plasmon resonance is excited, and as a consequence of the hole resonance enhanced EM field, there is an additional contribution to the magnetic plasmon modulation with respect to the equivalent continuous film, opening novel routes for the development of nonreciprocal architectures based on modified continuous magnetoplasmonic films.

2. Structure fabrication and characterization

The Au/Co/Au membrane was fabricated using a partial version [29] of the hole mask colloidal lithography technique [30] and magnetron sputter deposition. In brief, on top of a BK7 glass surface, a 200 nm thick PMMA and a 200 nm diameter polystyrene sphere layers were deposited by spin coating. Then a [(8 nm Au/2 nm Co)x4 /5 nm Au] multilayer was deposited by magnetron sputtering, and finally the spheres were removed by tape stripping. The 45 nm final membrane, see the sketch and the AFM image on Fig. 1, has a 3 holes/μm^2 hole concentration and a pore diameter of 200 nm. As a reference, a continuous multilayer film with equivalent thickness was deposited together with the membrane.
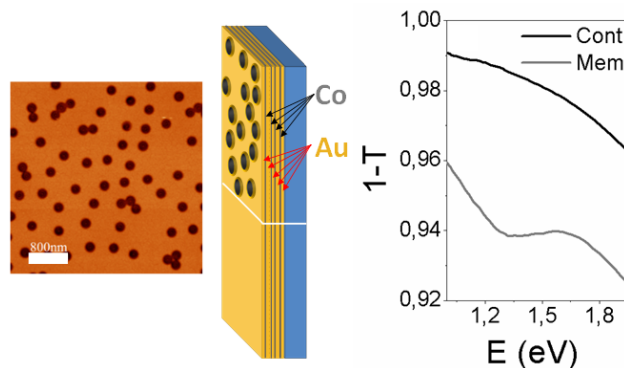

Fig. 1. AFM image (white scale line: 800 nm) of the membrane (left) and schematic view (centre) of the membrane (upper part) and the continuous films (lower part). Extinction spectra of the membrane (gray) and continuous layers (black) measured between 1 and 1.95 eV at normal incidence with a M200FI J.A, Woolam Co. TM ellipsometer (right).

Reflectivity, R, and transverse magneto-optical Kerr effect, ΔR/R, were measured as a function of the incident angle in Kretschmann configuration, using a p-polarized light of a supercontinuum laser. The spectral range was 0.95 eV-1.95 eV. In this configuration both localized and propagative SP modes are excited ΔR/R signal was generated in the transverse

magneto-optical Kerr (TMOKE) configuration using a coil that provides an oscillating magnetic field large enough to saturate the sample in both directions.

3. Results and discussion

First, in Fig. 1 we show extinction (1-T) spectra of both continuous and membrane layers. As it can be seen, the effect of incorporating holes into the continuous layer is twofold, with the logical increase of the transmittance and the appearance of a dip around 1.3 eV which is due to localized surface plasmons (LSP) associated to the holes [29].

In order to explore possible interactions between localized and propagating plasmons in the fabricated structures, measurements in attenuated total reflection were carried out. In Fig. 2(a) we show the angular dependence of the reflectivity for both structures at 1.3 eV.
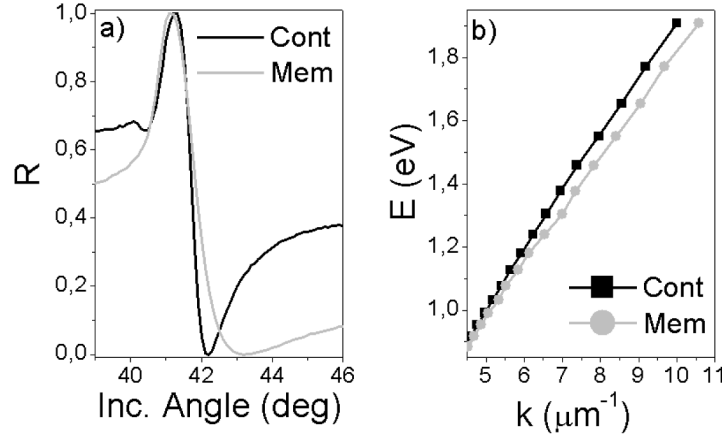

Fig. 2. (a) Normalized reflectivity at 1.3 eV for p-polarized light as a function of the incident angle for continuous (Cont) and membrane (Mem) layers (b) dispersion curves of both layers.

These curves are characterized by a resonant shape with maximum reflectivity at the total reflection angle, followed by a strong reduction of the reflectivity until a minimum is reached, corresponding to the optimum excitation of propagating surface plasmons (θ_{SP}). As it can be seen, the presence of holes in the membrane produces a shift towards larger incidence angles of this reflectivity minimum due to the reduced metallic character with respect to the continuous layer. Additionally, the holes also enhance the electron scattering in the metallic layer, which leads to a broadening of the minimum curve due to the increased losses. From this kind of measurements, and recording the angular position of the observed minima for different wavelengths, it is possible to obtain the dispersion curve of the excited propagating plasmons, see Fig. 2(b). As it can be seen, and compared with the continuous film curve, the dispersion curve of the membrane flattens i.e. the SPP modes become less dispersive, which is due to the presence of holes.

In order to determine the magnetic field induced modification of the SPP wavevector, similar measurements are carried out in the presence of a magnetic field in TMOKE configuration. In Figs. 3(b) and 3(c) we show the obtained results for continuous and membrane layers, respectively. In the angular region around the reflectivity minimum, the switching of the Co magnetization is equivalent to an angular derivative of the reflectivity. Therefore, the TMOKE signal ($\Delta R/R = (R(+ H)-R(-H))/R$), can be related to the angular derivative of the reflectance [5]:

$$\frac{\Delta R}{R} = \frac{\partial R}{\partial \theta} \frac{\Delta \theta}{R}. \tag{1}$$

Thus, the angular variation ($\Delta\theta$) can be obtained by comparing the intensity of the measured $\Delta R/R$ (black curves) signal with the angular derivative of R (red curves), see Figs.

3(b) and 3(c). Note that the angular derivative of R has contributions from both: the increase in the reflectivity at the total internal reflection angle (around 41 deg) and the decrease in the reflectivity due to the excitation of SPP (around 42 deg for the continuous layer and 43 deg for the membrane layer, respectively).
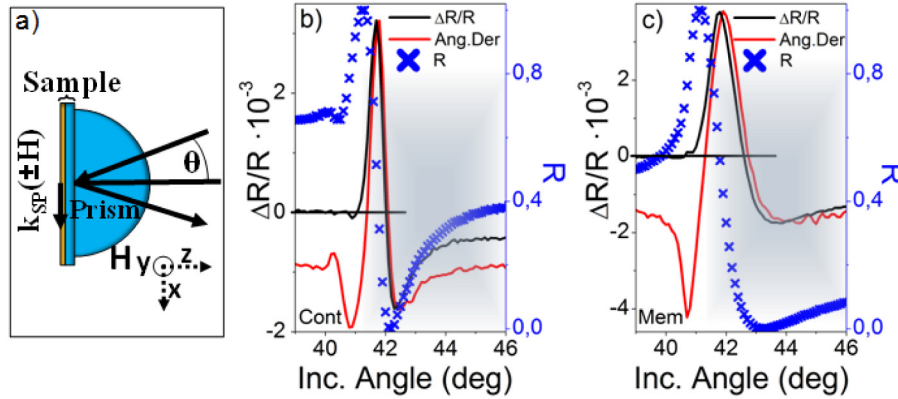

Fig. 3. (a) Sketch of the Kretschmann setup with the magnetic field (H) parallel to the sample surface. Normalized reflectivity (blue scattered) and the angular derivative curves $(\partial R/\partial\theta)(\Delta\theta/R)$ (red) compared to the measured $\Delta R/R$ spectra (black) of the continuous layer (b) and membrane (c) at 1.3 eV, where $\Delta\theta$ is a fitting parameter. The gray coloration shows the θ angle area where the plasmon coupling takes place separating from the vicinity of the total internal reflection angle.

Furthermore, the magnetic modulation of the excitation angle, $\Delta\theta$ is related to the magnetic field modulation of the wavevector as:

$$\left|\Delta k_{SP}\right| = \frac{\Delta\theta}{\tan\theta_{SP}} \cdot \left|k_{SP}\right|, \tag{2}$$

where $\left|k_{SP}\right| = k_0\sqrt{\varepsilon_p}\sin\theta_{SP}$, k_0 is the wavevector of the light and ε_p is the dielectric constant of the prism. Thus, the magnetic field wavevector modulations of the membrane and the continuous film were obtained by fitting the region corresponding to the excitation of SPP for all the measured photon energies. As it can be seen on Fig. 4(a), both curves follow a very similar trend except in the spectral region around 1.3 eV, where the hole plasmons are excited, and where an enhanced modulation is obtained. Worth to mention, in the studied membranes, the presence of an element characterized by a LSP and MO activity (the holes) produces an enhanced plasmon modulation with respect to the continuous films, contrary to what was previously obtained in similar systems in which the element responsible for the LSP was not magneto-optically active [26].

To understand the present results it is necessary to consider the physical processes that occur in this system, especially regarding the excitation of hole associated localized plasmons [31]. Such excitation produces an enhancement of the EM field in the metallic area surrounding the hole and, due to the interaction with the SPP, to the EM field of the SPP mode. Such EM enhancement induces the additional SPP wavevector magnetic modulation. In Fig. 4(b) we present the spectral dependence of the decay constant of the SPP modes for continuous and membrane layers calculated using the effective dielectric constants of the continuous and membrane layers obtained from ellipsometry measurements, whereas in Fig. 4(c) the intensity of the magnetic component of the EM field of the SPP mode at the interface between the metallic layer and air is also presented. As it can be observed, $|H_y|^2$ at the metal/air interface is very similar for both, continuous and membrane layers. On the other hand, a clear increase of the decay constant in the membrane layer is observed in the spectral region of the excitation of the hole LSP mode. Both facts indicate an increase of the EM field

intensity inside the membrane layer originated from the interaction between the LSP and SPP modes which is the origin of the enhancement of the wavevector modulation, inset of Fig. 4(a).
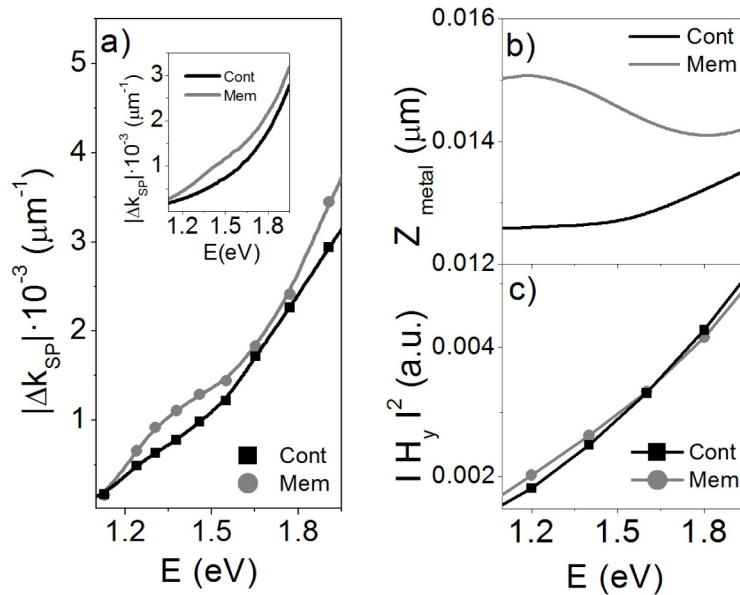

Fig. 4. (a) Experimental $|\Delta k_{SP}|$ curves of the membrane (gray points) and the continuous multilayer (black points) systems (the lines are shown as a guide for the eyes). Inset: calculated $|\Delta k_{SP}|$ curves (b) SPP decay constant in the metal (c) Intensity of the magnetic component of the EM field of the SPP mode ($|H_y|^2$) at the interface between the metallic layer and the air.

4. Conclusions

To conclude, we have shown that in magnetoplasmonic membranes, supporting MO active localized (LSP) and propagative SP (SPP) modes, an enhancement of magnetic field induced nonreciprocity effects occurs. Such enhancement is due to the modification induced in the EM field distribution of the SPP mode by the LSP mode. This proof of concept suggests novel approaches for the development of systems with enhanced nonreciprocal effects induced by nanostructuring continuous layers. For example, a way to further improve the magnetic field modulation of the wavevector could be to increase the EM enhancement by optimizing the concentration and hole size, and by changing the distribution of the ferromagnetic layer within the structure. This approach may be used in the development of innovative platforms for communications and sensing applications.